Brain Stimulation 15 (2022) 664–675

Contents lists available at ScienceDirect

Brain Stimulation

journal homepage: http://www.journals.elsevier.com/brain-stimulation

Simultaneous stereo-EEG and high-density scalp EEG recordings to study the effects of intracerebral stimulation parameters

S. Parmigiani [a, 1], E. Mikulan [a, 1], S. Russo [a, b], S. Sarasso [a], F.M. Zauli [a, b], A. Rubino [c], A. Cattani [d], M. Fecchio [e], D. Giampiccolo [f, g, h, i], J. Lanzone [j, k], P. D'Orio [c, l], M. Del Vecchio [l, m], P. Avanzini [l], L. Nobili [n, o], I. Sartori [c], M. Massimini [a, p, q], A. Pigorini [a, r, *]

[a] Department of Biomedical and Clinical Sciences "L. Sacco" Università degli Studi di Milano, Milan, Italy
[b] Department of Philosophy "Piero Martinetti", Università degli Studi di Milano, Milan, Italy
[c] "Claudio Munari" Epilepsy Surgery Centre, Azienda Socio Sanitaria Territoriale Grande Ospedale Metropolitano Niguarda, Milan, Italy
[d] Department of Mathematics & Statistics, Boston University, Boston, MA, USA
[e] Center for Neurotechnology and Neurorecovery, Department of Neurology, Massachusetts General Hospital, Boston, MA, USA
[f] Department of Neurosurgery, Department of Neuroscience, Biomedicine and Movement Sciences, University of Verona, Verona, Italy
[g] Department of Clinical and Experimental Epilepsy, UCL Queen Square Institute of Neurology, University College London, London, UK
[h] Victor Horsley Department of Neurosurgery, National Hospital for Neurology and Neurosurgery, Queen Square, London, UK
[i] Institute of Neurosciences, Cleveland Clinic London, London, UK
[j] Department of Systems Medicine, Neuroscience, University of Rome Tor Vergata, Rome, Italy
[k] Istituti Clinici Scientifici Maugeri, IRCCS, Neurorehabilitation Department of Milano Institute, Milan, Italy
[l] Istituto di Neuroscienze, Consiglio Nazionale delle Ricerche, Parma, Italy
[m] Department of Medicine and Surgery, Unit of Neuroscience, University of Parma, Parma, Italy
[n] Child Neuropsychiatry, IRCCS Istituto G. Gaslini, Genova, Italy
[o] Department of Neuroscience, DINOGMI, University of Genoa, Genoa, Italy
[p] Istituto Di Ricovero e Cura a Carattere Scientifico, Fondazione Don Carlo Gnocchi, Milan, Italy
[q] Azrieli Program in Brain, Mind and Consciousness, Canadian Institute for Advanced Research, Toronto, Canada
[r] Department of Biomedical, Surgical and Dental Sciences, University of Milano, Milan, Italy

ARTICLE INFO

Article history:
Received 17 November 2021
Received in revised form
6 April 2022
Accepted 6 April 2022
Available online 12 April 2022

Keywords:
Single pulse electrical stimulation
stereo-EEG
scalp hd-EEG
CCEP
Stimulation parameters

ABSTRACT

Background: Cortico-cortical evoked potentials (CCEPs) recorded by stereo-electroencephalography (SEEG) are a valuable tool to investigate brain reactivity and effective connectivity. However, invasive recordings are spatially sparse since they depend on clinical needs. This sparsity hampers systematic comparisons across-subjects, the detection of the whole-brain effects of intracortical stimulation, as well as their relationships to the EEG responses evoked by non-invasive stimuli.
Objective: To demonstrate that CCEPs recorded by high-density electroencephalography (hd-EEG) provide additional information with respect SEEG alone and to provide an open, curated dataset to allow for further exploration of their potential.
Methods: The dataset encompasses SEEG and hd-EEG recordings simultaneously acquired during Single Pulse Electrical Stimulation (SPES) in drug-resistant epileptic patients (N = 36) in whom stimulations were delivered with different physical, geometrical, and topological parameters. Differences in CCEPs were assessed by amplitude, latency, and spectral measures.
Results: While invasively and non-invasively recorded CCEPs were generally correlated, differences in pulse duration, angle and stimulated cortical area were better captured by hd-EEG. Further, intracranial stimulation evoked site-specific hd-EEG responses that reproduced the spectral features of EEG responses to transcranial magnetic stimulation (TMS). Notably, SPES, albeit unperceived by subjects, elicited scalp responses that were up to one order of magnitude larger than the responses typically evoked by sensory stimulation in awake humans.
Conclusions: CCEPs can be simultaneously recorded with SEEG and hd-EEG and the latter provides a reliable descriptor of the effects of SPES as well as a common reference to compare the whole-brain

DOI of original article: https://doi.org/10.1016/j.brs.2022.02.017.
* Corresponding author. Department of Biomedical and Clinical Sciences "L. Sacco" Università degli Studi di Milano, Milan, Italy.
E-mail address: andrea.pigorini@unimi.it (A. Pigorini).
[1] These two authors equally contributed.

https://doi.org/10.1016/j.brs.2022.04.007

effects of intracortical stimulation to those of non-invasive transcranial or sensory stimulations in humans.

1. Introduction

Intracortical electrical stimulation is an invaluable tool for surgical planning [1–3] and provides a direct assessment of brain evoked reactivity and effective connectivity in humans [4–6]. Clinical protocols often combine Single Pulse Electrical Stimulation (SPES) with stereotactic electroencephalography (SEEG) to evoke responses in areas explored with intracerebral electrodes [7,8]. Conceived for localizing the origin and diffusion of epileptogenic activity [9–12] in patients with focal drug-resistant epilepsy, SPES typically elicits consistent cortico-cortical evoked potentials (CCEPs) whose features reflect physiological and pathological characteristics of the underlying neural tissue [7–9,13,14].

Thanks to their high functional specificity [15], signal fidelity [16], and high spatial and temporal resolution [12–14], CCEPs can be used as an electrophysiological tool to assess brain reactivity and effective connectivity complementing functional and structural connectivity measures [4,13,17,18]. However, invasive recordings are necessarily sparse since intracerebral electrodes are typically circumscribed to a limited set of brain regions differing from one subject to another, depending on clinical needs [8,9,12,14,19]. The variability and sparsity of electrode placement clearly restricts a systematic comparison across subjects, the detection of the stimulation effects at the whole-brain level, as well as a direct comparison between CCEPs and other EEG potentials such as those evoked by non-invasive sensory, electrical, or magnetic stimulation [20].

The first aim of the present study was to overcome these limitations by simultaneously acquiring high-density EEG recordings, which provide a fixed observation point to reliably compare the responses evoked by SPES across subjects and to assess their amplitude and latency as well as their spectral properties at the scalp level. Specifically, we analyzed the effects induced by the systematic manipulation of different stimulation parameters on CCEPs recorded from both SEEG and scalp EEG during wakefulness. These included physical (pulse intensity and width), geometrical (angle and position with respect to white/grey matter) and topological (stimulated cortical area) stimulation parameters. The second aim was to describe the spectral properties of CCEPs evoked by the stimulation of different cortical areas at the hd-EEG level in order to validate previous findings obtained with Transcranial Magnetic Stimulation combined with scalp EEG (TMS-EEG), which showed a rostro-caudal gradient of the dominant frequency of the EEG response to TMS [21]. The third aim of the present study was to provide a first assessment of the absolute amplitude of the brain's response to clinical direct cortical stimulation recorded at the scalp, as compared to the typical magnitude of EEG responses recorded after sensory stimulation or TMS. Finally, to allow for more comprehensive data mining and a full exploration of the potential of simultaneous intracranial and scalp EEG recordings during SPES, we provide open access to the dataset reported here.

2. Materials and methods

2.1. Participants

A total of 36 patients (median age = 33 ± 8 years, 21 female, Table S1) from the "Claudio Munari" Epilepsy Surgery Center of Milan in Italy were enrolled in the study. All subjects had a history of drug-resistant, focal epilepsy, and were candidates for surgical removal/ablation of the seizure onset zone (SOZ). 31 patients did not show any anatomical malformation in the MRI, while the other 5 patients showed small anatomical alterations (see Table S1). All patients had no neurological or neuropsychological deficits. The investigated hemisphere/s and the electrodes' locations were decided based on electroclinical data and reported - for each subject - in Fig. S1. All patients provided their Informed Consent in accordance with the local Ethical Committee (ID 348-24.06.2020, Milano AREA C Niguarda Hospital, Milan, Italy) and with the Declaration of Helsinki.

2.2. Electrodes placement and localization

Electrode placement was performed as reported in Ref. [8] while electrode localization and anatomical labelling was performed as in Refs. [22,23]. Detailed descriptions can be found in Supplementary Materials.

2.3. Simultaneous SEEG and hd-EEG recordings

During the 1–3 weeks of hospitalization, SEEG activity was continuously recorded through a 192-channel recording system (NIHON-KOHDEN NEUROFAX-1200) with a sampling rate of 1000Hz. All acquisitions were referenced to two adjacent contacts located entirely in white matter [23]. During their last day of hospitalization all subjects included in the present study underwent simultaneous scalp non-invasive recordings by means of high-density Electroencephalogram (hd-EEG - 256 channels, Geodesic Sensor Net, HydroCel CleanLeads). Placement of the hd-EEG net on the head was performed by trained neurosurgeons using sterile technique, following a precise step-by-step protocol: (1) sterilization of the net, (2) removal of the protective bandage from the subject's head, (3) skin disinfection with Betadine and Clorexan, (4) positioning of the hd-EEG net, and (5) reduction of the impedances below 25–50 kOhm using conductive gel. An example of this setup is shown in Fig. 1. Hd-EEG was then recorded at 1000 Hz sampling rate using an EGI NA-400 amplifier (Electrical Geodesics, Inc; Oregon, USA) referenced to Cz. SEEG and hd-EEG recordings were aligned using a digital trigger signal generated by an external trigger box (EMS s.r.l., Bologna, Italy). At the end of the simultaneous data acquisition, the spatial locations of hd-EEG contacts and anatomical fiducials were digitized with a SofTaxicOptic system (EMS s.r.l., Bologna, Italy) and coregistered with a pre-implant 3D-T1 MRI. The net was then removed, and the skin was disinfected again.

2.4. Single Pulse Electrical Stimulation

During simultaneous hd-EEG and SEEG recordings, electrical single biphasic pulses (positive-negative) were injected between pairs of adjacent intracranial contacts pertaining to the same electrode with an inter-stimulus interval of at least 1 s across a wide range of intensities and pulse widths (see next paragraph). Brain activity was continuously recorded both from all other SEEG contacts as well as from the 256 scalp hd-EEG contacts. A single

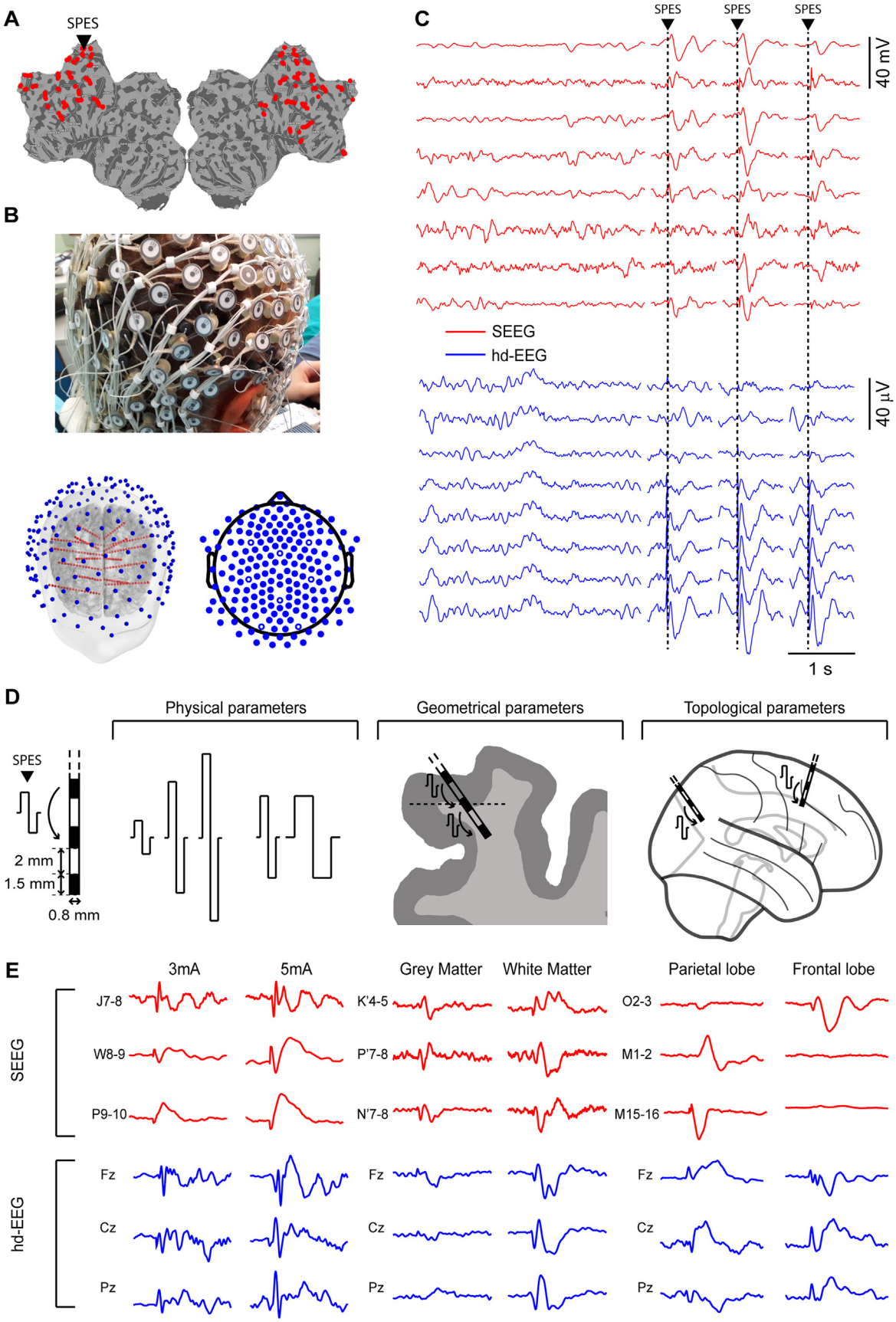

Fig. 1. Experimental setup. Panel A. Topographical representation, on a flatmap, of the SEEG contacts in one representative subject. The black triangle indicates the contact used for SPES (anterior cingulate). **Panel B**. Picture of simultaneous SEEG and hd-EEG recordings, 3D reconstruction of the brain and SEEG implant of one representative patient (same as A) and topographical representation of hd-EEG contacts. **Panel C**. Concurrent raw intracerebral SEEG (red) and hd-EEG (blue) signals recorded respectively from eight representative bipolar contacts and from eight scalp EEG contacts. The black triangle and dashed vertical line indicate the time at which SPES was delivered. **Panel D.** Left, outline of a multi-lead

stimulation session consisted of 30/40 consecutive trials. The number of sessions varied between subjects (9 ± 4). All the sessions included in the present work (N = 379) were selected following these criteria: stimulations (i) were delivered through a bipolar contact far from the SOZ (as indicated by electrical pathological activity and *a posteriori* confirmed by post-surgical assessment); (ii) were delivered through a bipolar contact that did not show spontaneous interictal epileptic activity (by visual inspection by P.dO., J.L., I.S.); (iii) did not elicit muscle twitches, somatosensory, or cognitive manifestations.

2.5. Physical, geometrical, and topological stimulation parameters

This work includes a dataset collected in the context of presurgical evaluation during which SPES was delivered based on clinical assessment, thus employing different stimulation parameters. Retrospectively, we decided to group these parameters into three categories, namely *physical*, *geometrical,* and *topological* (see Table S2).

Physical stimulation parameters included (i) stimulation intensity and (ii) pulse width. Stimulation intensities ranged from 0.1 mA to 5 mA. Specifically, SPES was delivered at 0.1 mA (n = 3), 0.5 mA (n = 1), 1 mA (n = 13), 3 mA (n = 63) and 5 mA (n = 243). Given the low number of sessions performed with intensities ≤1 mA we grouped them together (n = 17) and used these sessions only for the stimulation intensity analysis. Pulse widths were instead 0.5 ms (n = 184) or 1 ms (n = 139).

Geometrical stimulation parameters refer (i) to the position of the stimulating bipolar contact with respect to the interface between grey matter and white matter and (ii) to the angle of insertion of the SEEG electrode with respect to the cortical surface. To derive both parameters we used the 3D meshes of the grey and white matter obtained with Freesurfer [23]. The distance to the grey/white matter boundary was computed as the distance between the center of the stimulating bipolar contact and the closest point on the white matter mesh (see Figs. 1D and 3A) using the *trimesh* library. The distances of the bipolar contacts were then lumped into three categories: both contacts in grey matter (*GG*, n = 92), both contacts in white matter (*WW, n = 80*) and one contact in grey matter and one in white matter (*GW, n = 100*). The angle with respect to the cortical surface was calculated using the vector formed by the SEEG bipolar contact, and the normal vector of the closest segment of the white matter mesh (see Fig. S2). Then, the angles were lumped into two categories with respect to the cortical surface: *parallel* ($\delta < 45°$; $\delta > 315°$; and $135° < \delta < 225°$, n = 201) and *perpendicular* ($45° < \delta < 135°$ and $225° < \delta < 315°$, n = 71).

Topological stimulation parameters included the following stimulated cortical areas: Cingulate cortex (n = 30), Frontal cortex (n = 93), Insula (n = 26), Occipital cortex (n = 37), Parietal cortex (n = 113), Temporal cortex (n = 80) using the Desikan-Killiany atlas for the anatomical labelling [24].

2.6. Data pre-processing

The joint visual inspection of both SEEG and hd-EEG CCEPs allowed to retain 323/379 sessions (~85%), excluding 9 sessions that showed evoked epileptic spikes either at the scalp or intracerebral EEG level (Fig. S3, see also [12]), and 47 sessions characterized by a number of retained trials lower than 25 due to overall bad data quality or to the presence of interictal activity.

For the retained SPES sessions SEEG data were processed as in Ref. [25] while hd-EEG data were preprocessed as in Ref. [26]. Detailed procedures are reported in Supplementary Material.

2.7. Amplitude analysis

The effects of SPES parameters were assessed both at the SEEG and the hd-EEG level by measuring standard features of CCEP waveforms (amplitude and latency of N1 and N2) as well as surrogate measures of the overall response (Fig. 2). Specifically, at the SEEG level, the latter was quantified as the number of contacts responding with a significant CCEP (above 6 STD of the baseline, Fig. 2B) to SPES [27], while the amplitudes and latencies of N1 and N2 were obtained at the single contact level [28,29] and then averaged across contacts. Conversely, at the hd-EEG level, the overall response was obtained as the Global Mean Field Power (GMFP, between 0 ms and 500 ms, shaded blue area in Fig. 2B) and the amplitude and latencies of N1 and N2 were detected as the maximum peak of the GMFP (black circles in Fig. 2B), respectively in the 0–50 ms (dash and dot vertical line in Fig. 2) and 50 ms–300 ms time window. We used slightly different pipelines between scalp and intracranial recordings to make the measures comparable, as it was not possible to use the exact measures at both levels due to the intrinsic differences in the signals they record. SNR was calculated, both at the SEEG and at the hd-EEG level, as the ratio between the post stimulus activity included between 10 ms and 500 ms and the baseline (from −300 ms to −10 ms) of the contact showing the maximum post stimulus amplitude, expressed in dB (*i.e.*, 10*log10(Signal/Baseline)).

2.8. Spectral analysis

To validate the results of previous TMS-EEG studies [21], we compared the spectral properties of the CCEPs elicited by the stimulation of the occipital, parietal, and frontal cortices in order to assess the presence of a rostro-caudal gradient. For each session, we computed the Event Related Spectral Perturbations (ERSP [30]) and averaged them across contacts. The resulting average ERSPs were cumulated over time between 10 ms and 150 ms. Here, unlike TMS-EEG experiments [21], we characterized the dominant frequency as the mean frequency of the cumulated spectrum - instead of its peak frequency, as the latter is dominated by the stereotypical N1–N2 complex [29] evoked by intracranial electrical stimulation, e feature common to all stimulated sites (see also Figs. 6B and S8B).

2.9. Statistical analyses

Correlations between SEEG and hd-EEG measures were performed with non-parametric Spearman's correlation analyses. Differences among multiple groups were assessed with Kruskal-Wallis test (KW), followed by a post-hoc Wilcoxon Rank Sum test (WR, corrected for multiple comparisons using the False Discovery Rate method, FDR). Statistical interactions among stimulation parameters were performed with ANalysis Of VAriance (ANOVA). All descriptive values are reported along the manuscript as the mean ± standard deviation. Boxplots shown in the figures use standard parameters (25 & 75th percentiles and 1.5 * Inter Quartile

intracerebral electrode. Right, overview of stimulation parameters categories: physical, geometrical, and topological. **Panel E.** Examples of intracerebral SEEG (red) and hd-EEG (blue) signals recorded from representative bipolar contacts when delivering SPES with different physical (3 mA vs 5 mA), geometrical (white matter vs grey matter) and topological (parietal vs frontal lobe) parameters. (For interpretation of the references to colour in this figure legend, the reader is referred to the Web version of this article.)

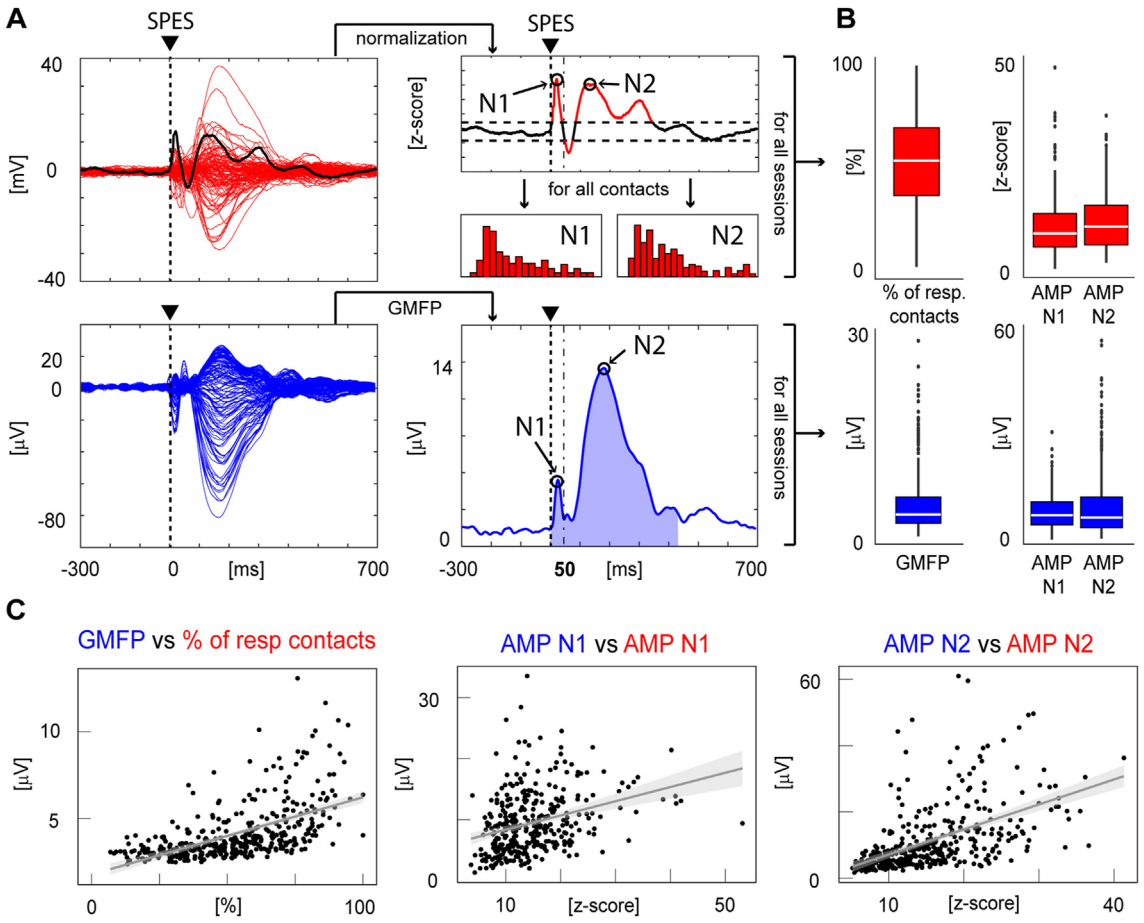

Fig. 2. Quantification procedures and comparisons of hd-EEG and SEEG responses to SPES. Panel A. Butterfly plots, N1 and N2 detections, GMFP calculations and quantifications of SEEG (top panel, traces in red) and hd-EEG (bottom panel, traces in blue) responses to SPES. *SEEG:* the same procedure was performed for each significant SEEG bipolar contact (*i.e.*, CCEP>6 STD of the baseline, as in Ref. [27]). After normalization (z-score) for the baseline (from −300 ms to −50 ms) and components detection (as in Refs. [39,40]), the amplitude of N1 and N2 components (black circles) were measured, obtaining two distributions (for N1 and N2). Values were then averaged across contacts to obtain average N1 and N2 amplitude values. *hd-EEG:* the GMFP is calculated from all hd-EEG contacts and then averaged between 0 ms and 500 ms (shaded blue area). The amplitude of N1 and N2 is detected as the maximum peak of the GMFP (black circles), respectively in the 0–50 ms (dash and dot vertical line) and 50 ms–300 ms time window. **Panel B.** In red, from left to right, percentage of responding contacts and N1 and N2 amplitudes for all sessions, recorded in SEEG. In blue, from left to right, GMFP voltage and N1 and N2 amplitudes, for all sessions, recorded in hd-EEG. **Panel C.** Linear regression analyses comparing hd-EEG (on y-axes) and SEEG measures (on x-axes). From left to right, linear regression between GMFP calculated at the hd-EEG level and the number of SEEG contacts responding to SPES with a significant CCEP ($r = 0.592$, $p < 0.001$); linear regression between the amplitude of N1 component calculated both at the hd-EEG and at the SEEG level ($r = 0.313$, $p < 0.001$); linear regression between the amplitude of N2 component calculated both at the hd-EEG and at the SEEG level ($r = 0.553$, $p < 0.001$). (For interpretation of the references to colour in this figure legend, the reader is referred to the Web version of this article.)

Range). All statistical analyses were performed in R. See Fig. S4 for a schematic overview of all the analyses performed.

2.9.1. The open dataset

All the preprocessed recordings are publicly available at the EBRAINS platform (https://ebrains.eu/) and at Open Science Framework (https://doi.org/10.17605/OSF.IO/WSGZP). The dataset is provided in BIDS format [31] and includes: simultaneous hd-EEG and SEEG from a total of 323 SPES sessions, obtained from 36 subjects (Table S1). In addition, it includes the spatial locations of the stimulating contacts in native MRI-space, MNI152-space and Freesurfer's surface-space, and the digitized positions of the 185 scalp EEG electrodes. It also contains the MRI of each subject, de-identified with AnonyMi [32]. Together with the dataset, a Jupyter Notebook to open the data is available at the following link: https://github.com/iTCf/ccepcoreg.

3. Results and discussion

To the best of our knowledge, this is the first time that responses to intracortical SPES were studied simultaneously with SEEG and scalp hd-EEG, as previous concurrent recordings were only carried out for spontaneous activity while using low-density standard 10–20 systems [33–38].

Here, simultaneous scalp hd-EEG and intracranial SEEG recordings of CCEPs were performed in 36 awake drug-resistant epileptic patients undergoing SPES for presurgical evaluation (see Fig. 1A-B-C). Overall, our dataset included 323 artefact-free recording sessions encompassing different stimulation parameters, which were clustered in three categories (see Fig. 1D): *physical* (stimulation intensity and pulse width), *geometrical* (position of the bipolar contact with respect to grey/white matter and angle of the electrode with respect to the cortical surface), and *topological* (stimulated cortical area). Importantly, the entire dataset is available at the EBRAINS platform (https://ebrains.eu/) and at Open Science Framework (https://doi.org/10.17605/OSF.IO/WSGZP) and includes not only simultaneous invasive and non-invasive

electrophysiological recordings but also individual de-identified MRIs. Beside the specific aim of the present manuscript, the provided dataset will allow not only to further compare electrophysiological recordings at different scales (*e.g.*, to test source localization algorithms) but also to investigate other factors involved in shaping the responses to intracranial stimulation – *e.g.,* anatomical features derived from the individual MRIs, structural connectivity from template coregistration, etc.

3.1. General features of CCEPs were consistent between SEEG and hd-EEG

CCEPs were highly reproducible from trial to trial, as assessed by the R^2 across trials, (SEEG = 0.4483 ± 0.1159; hd-EEG = 0.3225 ± 0.1513; Fig. 1C), and characterized by a high SNR both in intracerebral (SNR = 21.11 ± 5.01 dB) and in hd-EEG (SNR = 15.92 ± 4.18 dB) recordings (Fig. 1D). We first quantified the overall strength of the response to SPES by computing the GMFP (cumulated between 0 ms and 500 ms) at the hd-EEG level, and the percentage of significantly responding contacts at the SEEG level (Fig. 2B). Then, we evaluated the waveshape of CCEPs by measuring the average amplitude of N1 and N2 across all sessions (Fig. 2B and Methods). Despite displaying different waveshapes at the single contact level (see for example Fig. 1E), hd-EEG and SEEG showed on average a similar waveform characterized by a prominence of the typical [27,39–42] N1 and N2 components as shown in Fig. 2A. The average amplitude of N1 and N2 was, respectively, 9.5 ± 5.04 μV and 11.36 ± 9.86 μV for hd-EEG and 13.90 ± 7.04 z-value and 15.20 ± 7.02 z-value for SEEG. The corresponding average latencies of N1 and N2 were, respectively 16.79 ± 7.08 ms and 164.31 ± 48.39 ms for hd-EEG; and 8.31 ± 3.75 ms and 211.96 ± 70.95 ms for SEEG. Importantly, we found significant positive correlations between SEEG and hd-EEG in amplitude (GMFP and number of responding contacts, r = 0.592; N1 amplitude, r = 0.313; N2 amplitude, r = 0.553; all p < 0.001; Fig. 2C), but not in latency (N1 latency, r = 0.098; N2 latency, r = 0.087; Fig. S5A). Moreover, the correlations in amplitude, although significant, were far from complete. This suggests that, although general features of CCEPs could be captured at both levels, hd-EEG and SEEG are differently sensitive to physical, geometrical, and topological stimulation parameters, as confirmed by the analyses reported in the following paragraphs.

3.2. Physical stimulation parameters: the effects of pulse intensity and width

The effects of varying stimulation intensity could be appreciated in the CCEPs when measuring N1, N2 and overall strength of the response both at the SEEG and hd-EEG level (Fig. 3A). Statistical analysis performed with KW and post-hoc pairwise comparisons using WR tests revealed that the differences among the three stimulation intensities (≤1 mA, 3 mA and 5 mA) could be fully captured by both SEEG and hd-EEG (Fig. 3B). Specifically, SEEG showed a significant difference in the percentage of contacts responding to SPES ($H_{(2)} = 25.70$, $p < 0.001$), in the N1 amplitude ($H_{(2)} = 25.39$, $p < 0.001$) and in N2 amplitude ($H_{(2)} = 36.60$, $p < 0.001$). Similarly, hd-EEG showed significant differences in the GMFP ($H_{(2)} = 10.05$, $p = 0.006$), in N1 amplitude ($H_{(2)} = 12.13$, $p = 0.002$), as well as in N2 ($H_{(2)} = 11.95$, $p = 0.002$). Post-hoc statistical analyses are reported in Table S2. At odds with previous literature [43], we found no significant differences in latencies (Fig. S5) for different stimulation intensities; this was possibly due to the averaging of multiple latencies of N1 across SEEG contacts.

Conversely, differences in pulse width (0.5 ms vs 1 ms) were captured only by hd-EEG but not by SEEG (Fig. 3C). Specifically, at the hd-EEG level, WR tests showed that GMFP, amplitude of N1 and amplitude of N2 were significantly larger for 1 ms than for 0.5 ms pulse width (W = 14193, W = 13916, W = 12663, respectively, all $p < 0.001$; Fig. 3D). No significant differences were observed in latencies (Fig. S5). Of note, both physical stimulation parameters (intensity and width) were not biased by any specific spatial distribution (see Figs. S3A–B).

Overall, these results are in line with previous intracerebral studies which demonstrated that the amplitude of N1 and N2 components and, more in general, the amplitude of CCEPs depend on the amount of injected current [44–47]. However, while the effect of stimulation intensity has been clearly described, the effects of pulse width are less consistent across the literature [14,30,46,48]. Here, the larger hd-EEG responses elicited by longer pulse width stimulations may suggest the involvement of a larger network, implying broader polysynaptic activations [28] and recurrent activities [25,49]. In summary, complementing intracerebral explorations with whole brain hd-EEG measures confirms previous findings regarding stimulation intensity and suggests that the effects of pulse width may not be fully captured by SEEG recording alone.

3.3. Geometrical stimulation parameters: the effects of contact position with respect to the cortex

First, we assessed the SEEG and hd-EEG responses to SPES when stimulating at different distances from grey-white matter interface (operationalized as GG/GW/WW; Fig. 4A). We observed that this geometrical stimulation parameter affected CCEPs both at the SEEG and hd-EEG level, as assessed by KW statistical analyses. Specifically, this was true for all measures at the hd-EEG level (for GMFP, $H_{(2)} = 15.03$, $p < 0.001$; for AMP N1, $H_{(2)} = 26.41$, $p < 0.001$; for AMP N2 $H_{(2)} = 11.95$, $p < 0.01$). Instead, at the SEEG level only the percentage of responding contacts and the amplitude of N2 showed a significant difference ($H_{(2)} = 12.66$, $p < 0.01$; $H_{(2)} = 17.47$, $p < 0.001$; respectively), while the N1 amplitude was not significantly affected ($H_{(2)} = 5.12$, $p = 0.077$). In particular, except for N1 in SEEG, post-hoc comparisons showed that the stimulation of WW was more effective (*i.e.,* larger CCEP response) with respect to the stimulation of GW, which in turn was more effective than the stimulation of GG (Fig. 4B and Table S3). In line with this we also found that latencies of both N1 and N2 were shorter when stimulating white matter (GG > GW > WW, Fig. S5D). Of note, this was observed only with hd-EEG and not with SEEG.

The second geometrical parameter we considered was the angle with respect to the grey-white matter interface (operationalized as parallel/perpendicular, Fig. 4C). In this case (Fig. 3C), perpendicular stimulations led to significantly larger responses only at the hd-EEG level (for GMFP, W = 6361 $p = 0.045$; for AMP N1 W = 6483 $p = 0.038$; for AMP N2 W = 6551 $p = 0.044$). On the contrary, none of the SEEG measures showed significant differences (W = 6588 $p = 0.125$, W = 5491 $p = 0.473$, and W = 5491 $p = 0.286$ for the percentage of responding contacts, AMP N1, and AMP N2, respectively). No significant differences were observed in latencies (Fig. S5). Of note, both geometrical parameters (white matter distance and angle) were not biased by any specific spatial distribution (Figs. S3C–D).

Studies on intracerebral techniques that focused on the effect of geometrical stimulation parameters have been performed to optimize Deep Brain Stimulation protocols. According to these studies, small differences in electrode location [50–53], as well as orientation [54] can generate considerable differences in the activated white matter pathways. In line with these findings, the larger and faster (Fig. S5) hd-EEG responses observed both with WW and

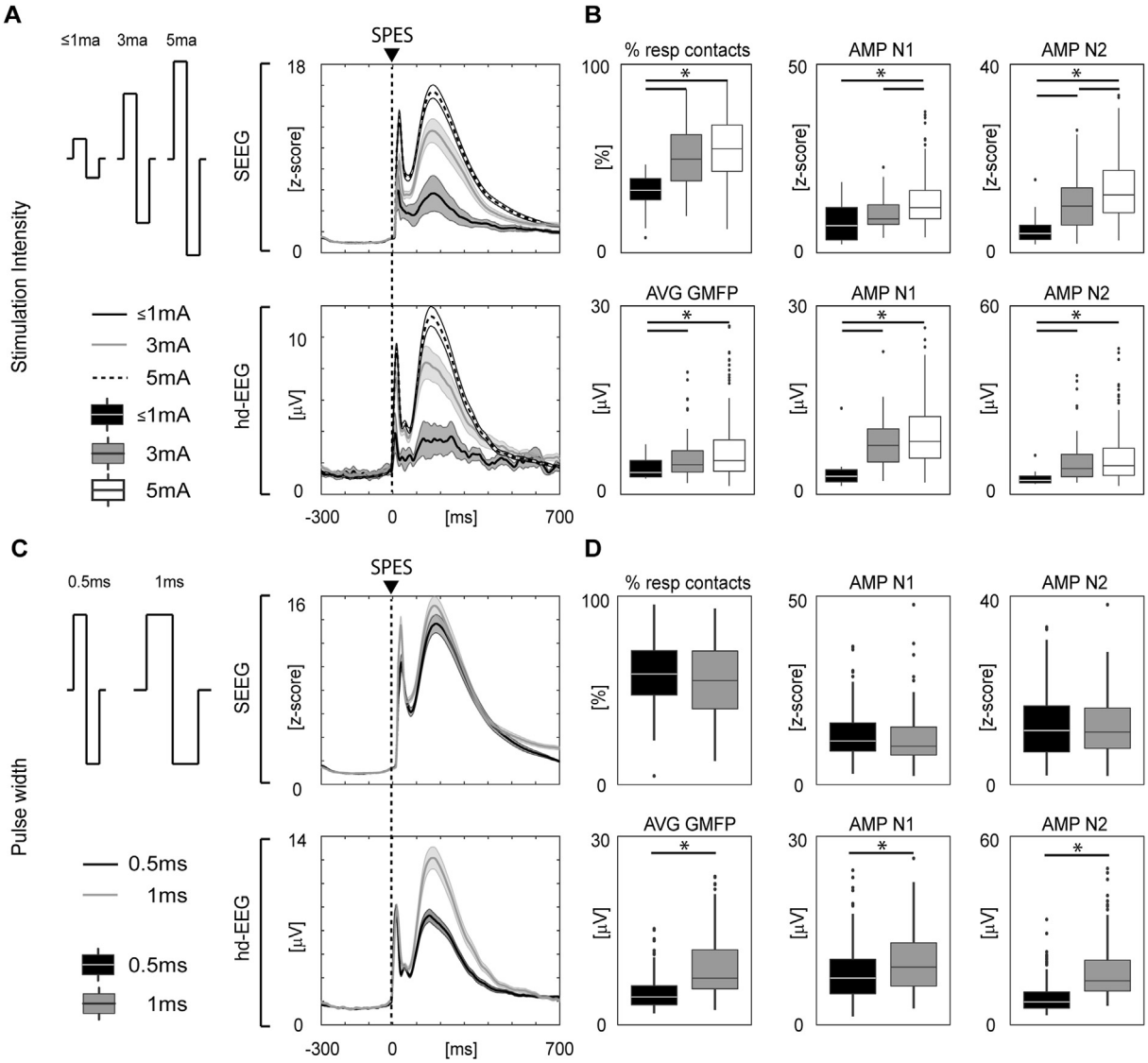

Fig. 3. hd-EEG and SEEG responses to SPES delivered at different physical stimulation parameters: intensities and pulse durations. Panel A. Left, outline of the different pulse intensities; right, grand average of data obtained from all the subjects and sessions. **Panel B**. *Upper line*: from left to right, percentage of responding contacts and N1 and N2 amplitudes for all sessions, recorded in SEEG. *Lower line:* from left to right, GMFP voltage and N1 and N2 amplitudes, for all sessions, recorded in hd-EEG. Asterisks indicate significant statistical differences (post-hoc, two-tailed WR, $p < 0.01$, FDR corrected). **Panel C**. Left, outline of the different pulse durations; right, grand average of data obtained from all the subjects and sessions. **Panel D.** *Upper line*: from left to right, percentage of responding contacts and N1 and N2 amplitudes for all sessions, recorded in SEEG. *Lower line:* from left to right, GMFP voltage and N1 and N2 amplitudes, for all sessions, recorded in hd-EEG. Asterisks indicate significant statistical differences (WR, $p < 0.01$, FDR corrected).

perpendicular stimulations could be ascribed to the more extensive involvement of white-matter fiber bundles.

3.4. Interactions between physical and geometrical stimulation parameters

The above-mentioned stimulation parameters could in principle interact at different levels. However, a model with the interaction of all the explored physical and geometrical parameters would require a larger sample. For this reason, we tested the interactions using pairwise bivariate ANOVAs. Overall, we observed significant interactions only at the hd-EEG level in pulse width/angle, pulse width/distance from white matter, intensity/distance from white matter (Fig. S9). Specifically, the first two were found both for GMFP and amplitude of N2 while the latter was found only for N1 amplitude. Although it is conceivable that longer pulse widths and higher intensities might have stronger effects when delivered closer or perpendicular to white matter fiber bundles [55–57], future studies including a larger sample size and a multivariate analysis will be needed to reach an exhaustive interpretation of these interactions. However, the fact that these results were only observable from the scalp again demonstrates the value of simultaneous recordings, and their capacity to uncover effects that might have otherwise remained undetected due to spatial limitations.

3.5. Topological stimulation parameters: the effect of stimulating different areas

Further, we evaluated whether the stimulation of different cortical areas was associated with differences in CCEP amplitude. At the hd-EEG level, we systematically observed that responses to the stimulation of the frontal cortex were larger than those obtained when stimulating any other cortical area. Specifically, as shown in Fig. 5C, KW test and Wilcoxon Rank Sum post-hoc pairwise

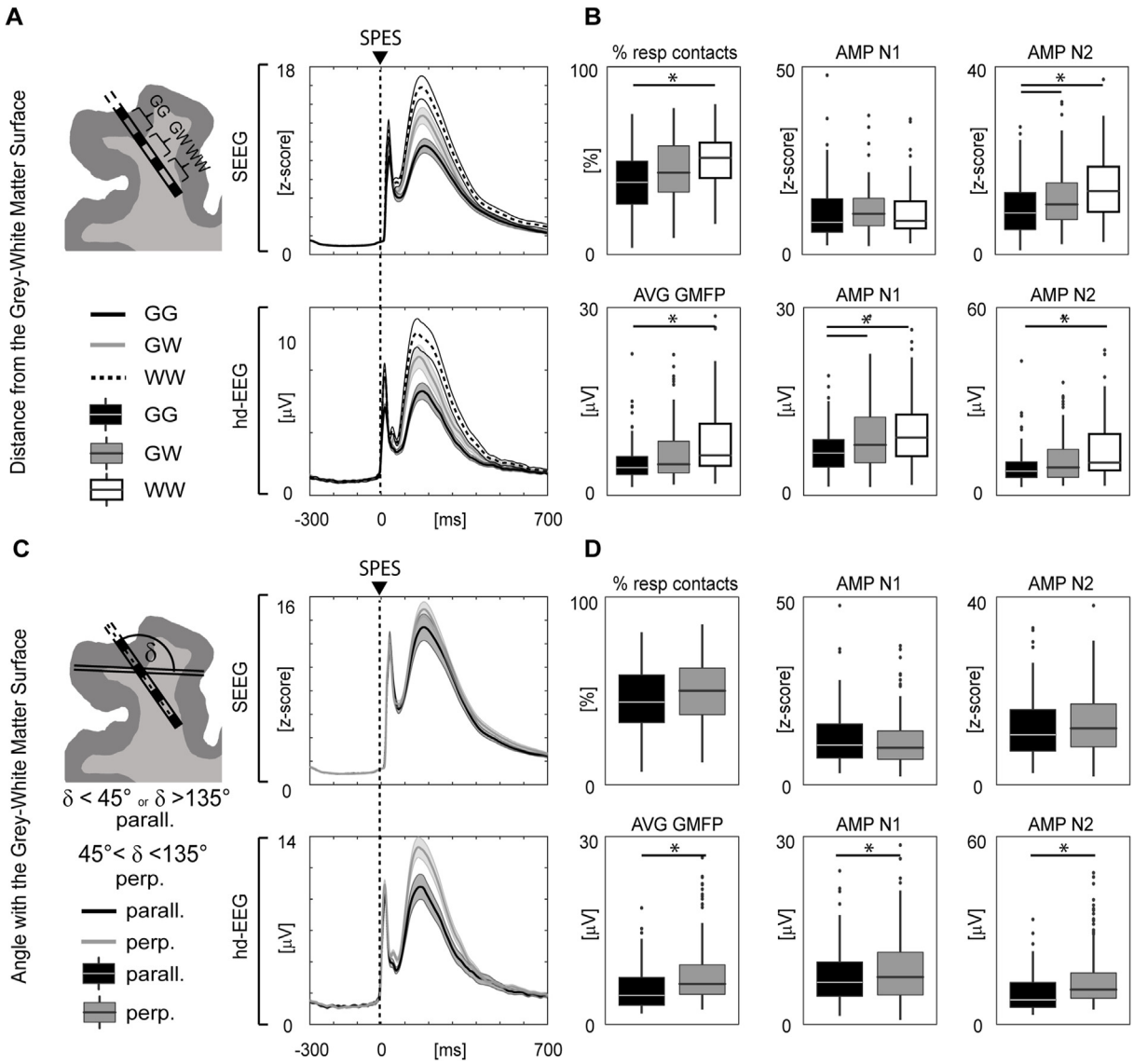

Fig. 4. Hd-EEG and SEEG responses to SPES delivered at different geometrical stimulation parameters. Panel A. Left, outline of the distance from the grey-white matter surface (G and W respectively); right, grand average of data obtained from all the subjects and sessions. **Panel B**. *Upper line*: from left to right, percentage of responding contacts and N1 and N2 amplitudes for all sessions, recorded in SEEG. *Lower line:* from left to right, GMFP voltage and N1 and N2 amplitudes, for all sessions, recorded in hd-EEG. Asterisks indicate significant statistical differences (post-hoc, two-tailed WR, $p < 0.01$, FDR corrected). **Panel C**. Left, outline of the angle with respect to the grey-white matter surface (parallel, perpendicular); right, grand average of data obtained from all the subjects and sessions. **Panel D.** *Upper line*: from left to right, percentage of responding contacts and N1 and N2 amplitudes for all sessions, recorded in SEEG. *Lower line:* from left to right, GMFP voltage and N1 and N2 amplitudes, for all sessions, recorded in hd-EEG. Asterisks indicate significant statistical differences (WR, $p < 0.01$, FDR corrected).

comparisons revealed a significant difference for all the measures at the hd-EEG level (GMFP: $H_{(5)} = 15.45$, $p = 0.008$; AMP1 $H_{(5)} = 20.32$, $p = 0.001$; AMP2 $H_{(5)} = 19.85$, $p = 0.001$). On the contrary, among all the considered SEEG measures, only N1 showed a significant effect (percentage of responding contacts: $H_{(5)} = 10.41$, $p = 0.06$; AMP1 $H_{(5)} = 20.71$, $p = 0.0009$; AMP2 $H_{(5)} = 9.29$, $p = 0.09$). Post-hoc statistical analyses are reported in Table S5. Importantly, at the hd-EEG level none of the reported measures correlated with the depth of SPES site (Fig. S6). Of note, differences in latency were observed only at the hd-EEG level, where we found that the stimulation of cingulate, temporal, and insular cortices lead to longer N1 latencies with respect to the stimulation of occipital, frontal, and parietal cortices (Fig. S5F). All these results require cautious interpretation since the physical and geometrical stimulation parameters were not completely balanced between cortices; a larger dataset will be needed to derive more robust conclusions. However, the high-amplitude responses to SPES of the frontal cortex could be due to the direct engagement of anterior circuits related to saliency [58,59], which are thought to be responsible for the generation of high amplitude scalp EEG graphoelements such as the K-complex [60] and the Vertex Wave [58,61]. Intriguingly, the latter is the largest graphoelement that can be evoked by sensory stimulation in an awake brain and is on average 25 μV, with a peak-to-peak maximal amplitude of 35 μV [58–62].

3.6. Comparing invasive and non-invasive brain stimulation techniques

In our dataset, CCEPs voltage at Cz were on average 43.42 μV (average reference; 53.1 μV when referenced to mastoid), reaching

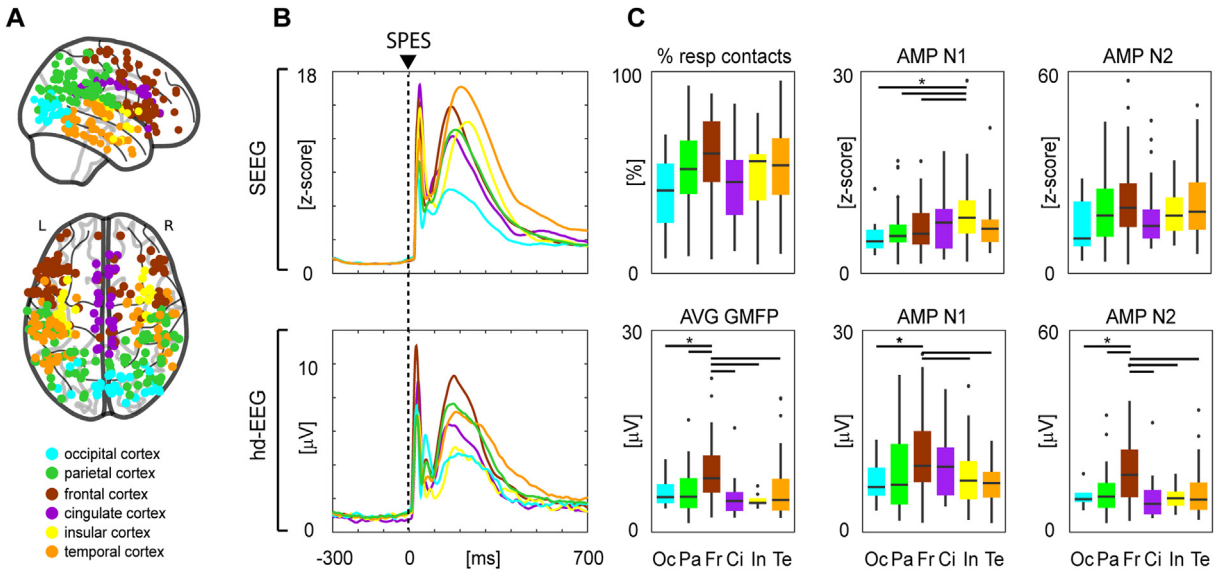

Fig. 5. Hd-EEG and SEEG responses to SPES delivered through contacts in different cortices (topological parameters). Panel A. Topographical distribution of the stimulations performed through bipolar SEEG contacts located in different cortical areas (cingulate cortex, insula, frontal cortex, occipital cortex, parietal cortex, temporal cortex). Color coding is consistent across the figure. **Panel B.** Grand average across sessions and subjects of the GMFP obtained by SPES of all the six cortices reported in Panel A; dashed vertical line indicates SPES timing. Here and across the figure, top panels refer to SEEG recordings, while bottom panels refer to hd-EEG recordings. **Panels C.** From left to right, boxplots of average GMFP amplitude of N1 and amplitude of N2. Asterisks indicate significant statistical differences obtained with a post-hoc, two-tailed WR test ($p < 0.05$, FDR corrected). (For interpretation of the references to colour in this figure legend, the reader is referred to the Web version of this article.)

a peak-to-peak maximum of 172.16 μV (average reference; 214.43 μV when referenced to mastoid), and thus much larger than any sensory evoked potential recorded during wakefulness. Indeed, sensory (auditory, somatosensory, or visual) evoked potentials may range from a fraction of a microvolt to few microvolts [62–64]. This finding is particularly interesting when considering CCEPs impact on the subjects' awareness: despite eliciting massive and long-lasting activations of cortical circuits, none of our intracranial stimulation resulted in any reportable perceptual event.

Interestingly, CCEPs' voltages at the scalp EEG level were also consistently larger as compared to TMS evoked potentials (TEPs), which typically attain amplitudes of about 20 μV [62–65]. At the same time, our results showed that, similarly to TMS, SPES could elicit large EEG components that persist for hundreds of

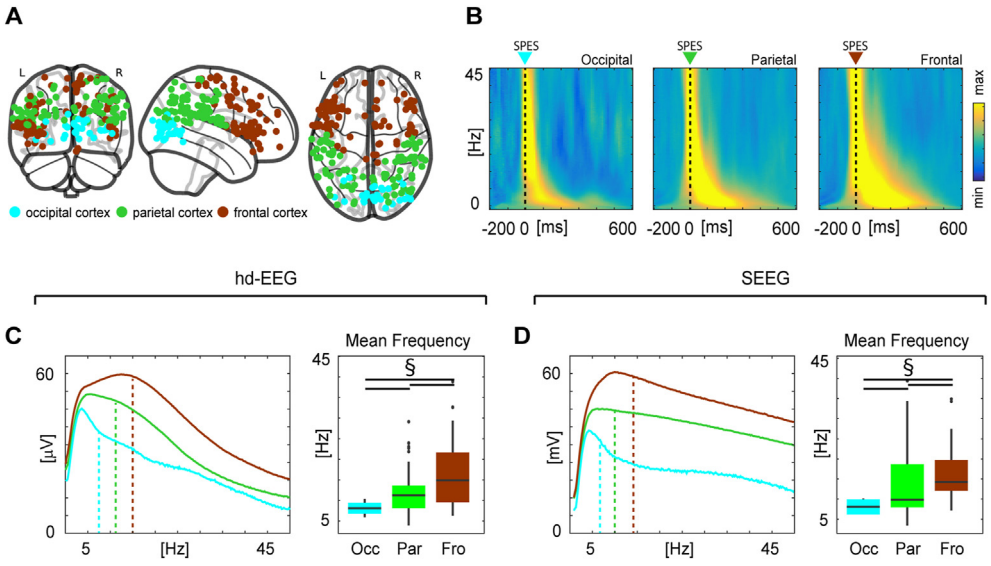

Fig. 6. Reproducing TMS-EEG experiments: rostro-caudal gradient of cortical spectral features. Panel A. Topographical distribution of the stimulations performed through bipolar SEEG contacts located in different cortices (occipital cortex, parietal cortex, frontal cortex). Color coding is consistent across the figure. **Panel B.** The spectral properties (ERSP) emerged at the whole brain level after SPES in the three different sites (occipital, parietal, frontal), recorded with hd-EEG. **Panel C** concerns hd-EEG recordings. *Left.* Grand average across sessions and subjects of spectral profile, namely ERSPs cumulated over time (between 5 ms and 150 ms), obtained by SPES of occipital, parietal, and frontal cortices; dashed vertical lines indicate mean frequencies. *Right.* Boxplot of the mean frequency for occipital, parietal, and frontal cortices. § indicates significant statistical differences ($p < 0.05$) obtained with one-tailed Wilcoxon test, under the assumption that the mean frequency of occipital, parietal and frontal cortex are characterized by a rostro-caudal gradient [21]. **Panel D.** Same as C but concerning SEEG recordings. (For interpretation of the references to colour in this figure legend, the reader is referred to the Web version of this article.)

milliseconds, thus corroborating the idea that late components genuinely reflect the effects of direct cortical rather than peripheral activation [66]. More importantly, combining hd-EEG with SPES allowed to directly compare invasive and non-invasive (TMS) stimulation methods in terms of spectral properties emerging at the local and at whole brain level when perturbing the brain at different sites - as in TMS-EEG investigations [21]. This was done by computing time-frequency spectra (ERSP) of the CCEPs collected with SEEG and hd-EEG when stimulating occipital, parietal, or frontal cortices (Fig. 6A and B). Cumulating these ERSPs over time (between 5 ms and 150 ms) resulted in a spectral profile for each stimulus location, whose grand average is depicted in Fig. 6C and D. This analysis showed that the CCEPs evoked by the stimulation of the occipital, parietal and frontal cortices were characterized by a rostro-caudal gradient of mean frequencies - *i.e.,* occipital < parietal < frontal (Fig. 6C and D). These differences were significant both at the hd-EEG and at the SEEG level as assessed by KW tests (hd-EEG: $H_{(2)} = 16.49$, $p = 0.0002$; SEEG: $H_{(2)} = 8.31$, $p = 0.013$) and post-hoc one-tailed WR tests (Table S5). We also conducted an additional analysis on the main frequencies of the cingulate, insular, and temporal cortices, which is reported in the supplementary materials (Fig. S8). These results, obtained with a very different kind of perturbation (intracortical SPES), confirm previous observations obtained with TMS-EEG [21,61] and generalize the notion of a specific frequency-tuning, *i.e.,* the natural frequency of cortical circuits.

3.7. Limitations

Our results were obtained from a population of epileptic patients whose clinical condition and specific treatment [67,68] may affect both invasive and non-invasive recordings. To minimize such confound, we did not include any SEEG contact located in the SOZ (as verified by surgical resection) or exhibiting sustained pathological interictal activity. Moreover, we excluded from the analyses all the CCEPs showing evoked epileptic activity at the SEEG and/or at the hd-EEG level [9].

Clinical needs also constrained the exploration of physical stimulation parameters to few pulse intensities and two pulse widths. Future studies encompassing multiple intensity and pulse width steps, like the one by Paulk and colleagues [69], will allow for a more systematic comparison between invasive and non-invasive stimulation techniques.

In this study we focused on the direct comparison between scalp and intracranial signals. To make their signals comparable we employed analogous measures across recording types, but these measures were not identical. An interesting strategy for future studies would be to perform source localization on hd-EEG data and not only assess its concordance with respect to SEEG but also extend the analysis to areas not sampled by intracranial explorations.

Finally, the combination of SEEG and hd-EEG entails specific data acquisition protocols to prevent infective risks. This implies a short duration of SPES procedures and thus the acquisition of few trials from a limited number of sites per patient. To compensate for these constraints, we verified that the number of acquired trials led to reliable responses in terms of SNR - both at the SEEG and hd-EEG level - and we included a relatively large number of stimulation sessions ($N = 323$) and subjects ($N = 36$). This sample size allowed to perform univariate analyses and to assess interactions through bivariate models (Fig. S9). Larger datasets will ensure the possibility of performing multivariate analyses considering all the explored variables and will allow to derive more robust and fine-grained topological conclusions with balanced physical and geometrical properties across sites. Increasing the size of the dataset will also allow to probe the differential contribution of specific brain structures (*e.g.*, deep vs superficial areas) in shaping the regional aspects of hd-EEG responses to a direct perturbation. In this respect, the results shown in the present manuscript represent a first step toward a more comprehensive description of the scalp EEG responses to SPES and their relationship with intracerebral recordings.

4. Conclusions

The present results show that CCEPs recorded with hd-EEG are overall aligned with those obtained with invasive SEEG recordings. Most important, they show that macroscale hd-EEG recordings are exquisitely sensitive to variations in stimulation parameters, including local changes in physical and geometrical stimulus properties, while overcoming the limitations typical of sparse recordings. Specifically, hd-EEG allowed capturing differences in amplitude and latency that were not detected by SEEG alone, thus suggesting that complementing invasive techniques with whole brain recordings can uncover effects that might have otherwise remained undetected.

In general, the possibility of studying and comparing across subjects the effects of multiple local intracortical perturbations at the whole brain level opens interesting fields of investigations. For example, it could provide the broad spatial coverage and cross-subject reference point required to study high-level cognitive functions, which usually recruit a widespread network of regions [20]. Additionally, it may complement current datasets on the structural [70] and functional [71] connectomes with an effective connectome [40] whereby intracortical interactions are systematically studied by a causal perspective in the common recording space of scalp EEG and with a full assessment of spatio-temporal dynamics. Moreover, hd-EEG recordings allow direct comparisons between CCEPs and other potentials elicited by non-invasive stimulation. For example, EEG responses to SPES reproduced the rostro-caudal spectral gradient as previously shown by TMS-EEG measurements. An intriguing finding is that SPES evoked responses that were systematically larger than any sensory evoked potential that can be elicited during wakefulness. This is particularly notable considering the fact that none of the stimulation included in this study elicited any perceptual event.

Along these lines, future studies involving SPES and hd-EEG - coupled with more ecological stimuli - should investigate why some brain responses are associated with perceptual events whereas others, despite being larger and long lasting, are not.

Funding

This research has received funding from the European Union's Horizon 2020 Framework Programme for Research and Innovation under the Specific Grant Agreement No. 720270 (Human Brain Project SGA1- to M.M.), No. 785907 (Human Brain Project SGA2 - to M.M. and P.A.), and No. 945539 (Human Brain Project SGA3 - to M.M. and P.A.). The study has also been partially funded by the grant "Sinergia" CRSII3_160803/1 of the Swiss National Science Foundation (to M.M.) and the Tiny Blue Dot Foundation (to M.M.).

CRediT authorship contribution statement

S. Parmigiani: Conceptualization, Data collection, Formal analysis, Writing – original draft, Writing – review & editing. **E.P. Mikulan:** Conceptualization, Formal analysis, Writing – original draft, Writing – review & editing. **S. Russo:** Conceptualization, Data collection, Formal analysis, Writing – original draft, Writing – review & editing. **S. Sarasso:** Writing – original draft, Writing – review & editing. **F.M. Zauli:** Data collection, Writing – review &

editing. **A. Rubino:** Data collection, Writing – review & editing. **A. Cattani:** Formal analysis, Writing – review & editing. **M. Fecchio:** Formal analysis, Writing – review & editing. **D. Giampiccolo:** Investigation, Writing – review & editing. **J. Lanzone:** Investigation, Writing – review & editing. **P. D'Orio:** Investigation, Writing – review & editing. **M. del Vecchio:** Writing – review & editing. **P. Avanzini:** Writing – review & editing. **L. Nobili:** Writing – review & editing. **I. Sartori:** Data collection, Investigation, Writing – review & editing. **M. Massimini:** Supervision, Writing – review & editing. **A. Pigorini:** Conceptualization, Supervision, Data collection, Formal analysis, Writing – original draft, Writing – review & editing.

Declarations of competing interest

None of the authors have conflicts of interest to disclose in relationship with the current work.

Acknowledgements

We are grateful to Mario Rosanova, Susanna Bianchi, Jacopo Favaro, Michela Solbiati, Aurora Sium, Alessandro Viganò, Renzo Comolatti, Giulia Furregoni, Michele Colombo and Martina Revay for their comments and suggestions.

Appendix A. Supplementary data

Supplementary data to this article can be found online at https://doi.org/10.1016/j.brs.2022.04.007.

References

[1] Foerster O, Altenburger H. Elektrobiologische Vorgänge an der menschlichen Hirnrinde. Dtsch Z für Nervenheilkd 1935;135:277–88.
[2] Krause F. Die operative behandlung der epilepsie. Med Klin 1909;5:1418–22.
[3] Yamao Y, Matsumoto R, Kunieda T, Arakawa Y, Kobayashi K, Usami K, et al. Intraoperative dorsal language network mapping by using single-pulse electrical stimulation: intraoperative Language Network Mapping. Hum Brain Mapp 2014;35:4345–61. https://doi.org/10.1002/hbm.22479.
[4] David O, Bastin J, Chabardès S, Minotti L, Kahane P. Studying network mechanisms using intracranial stimulation in epileptic patients. Front Syst Neurosci 2010;4. https://doi.org/10.3389/fnsys.2010.00148.
[5] Selimbeyoglu A, Parvizi J. Electrical stimulation of the human brain: perceptual and behavioral phenomena reported in the old and new literature. Front Hum Neurosci 2010;4:46.
[6] Fox KC, Foster BL, Kucyi A, Daitch AL, Parvizi J. Intracranial electrophysiology of the human default network. Trends Cognit Sci 2018;22:307–24.
[7] Cossu M, Cardinale F, Castana L, Citterio A, Francione S, Tassi L, et al. Stereoelectroencephalography in the presurgical evaluation of focal epilepsy: a retrospective analysis of 215 procedures. Neurosurgery 2005;57:706–18. https://doi.org/10.1227/01.NEU.0000176656.33523.1e.
[8] Cardinale F, Rizzi M, Vignati E, Cossu M, Castana L, D'Orio PG, et al. Stereoelectroencephalography: retrospective analysis of 742 procedures in a single centre surgical series. Brain 2019;142(9). https://doi.org/10.1093/brain/awz196.
[9] Valentin A. Responses to single pulse electrical stimulation identify epileptogenesis in the human brain in vivo. Brain 2002;125:1709–18. https://doi.org/10.1093/brain/awf187.
[10] Parvizi J, Kastner S. Promises and limitations of human intracranial electroencephalography. Nat Neurosci 2018;21:474–83. https://doi.org/10.1038/s41593-018-0108-2.
[11] Alarcón G, Jiménez-Jiménez D, Valentín A, Martín-López D. Characterizing EEG cortical dynamics and connectivity with responses to single pulse electrical stimulation (SPES). Int J Neural Syst 2018;28:1750057. https://doi.org/10.1142/S0129065717500575.
[12] Valentín A, Alarcón G, Honavar M, García Seoane JJ, Selway RP, Polkey CE, et al. Single pulse electrical stimulation for identification of structural abnormalities and prediction of seizure outcome after epilepsy surgery: a prospective study. Lancet Neurol 2005;4:718–26. https://doi.org/10.1016/S1474-4422(05)70200-3.
[13] Keller CJ, Bickel S, Entz L, Ulbert I, Milham MP, Kelly C, et al. Intrinsic functional architecture predicts electrically evoked responses in the human brain. Proc Natl Acad Sci Unit States Am 2011;108:10308–13. https://doi.org/10.1073/pnas.1019750108.
[14] Matsumoto R, Kunieda T, Nair D. Single pulse electrical stimulation to probe functional and pathological connectivity in epilepsy. Seizure 2017;44:27–36.
[15] Schalk G, Kubanek J, Miller KJ, Anderson NR, Leuthardt EC, Ojemann JG, et al. Decoding two-dimensional movement trajectories using electrocorticographic signals in humans. J Neural Eng 2007;4:264.
[16] Ball T, Kern M, Mutschler I, Aertsen A, Schulze-Bonhage A. Signal quality of simultaneously recorded invasive and non-invasive EEG. Neuroimage 2009;46:708–16.
[17] Keller CJ, Honey CJ, Mégevand P, Entz L, Ulbert I, Mehta AD. Mapping human brain networks with cortico-cortical evoked potentials. Phil Trans R Soc B 2014;369:20130528. https://doi.org/10.1098/rstb.2013.0528.
[18] Silverstein BH, Asano E, Sugiura A, Sonoda M, Lee M-H, Jeong J-W. Dynamic tractography: integrating cortico-cortical evoked potentials and diffusion imaging. Neuroimage 2020;215:116763.
[19] Scorza D, Amoroso G, Cortés C, Artetxe A, Bertelsen Á, Rizzi M, et al. Experience-based SEEG planning: from retrospective data to automated electrode trajectories suggestions. Healthc Technol Lett 2018;5:167–71.
[20] Johnson EL, Kam JW, Tzovara A, Knight RT. Insights into human cognition from intracranial EEG: a review of audition, memory, internal cognition, and causality. J Neural Eng 2020;17(5):051001.
[21] Rosanova M, Casali A, Bellina V, Resta F, Mariotti M, Massimini M. Natural frequencies of human corticothalamic circuits. J Neurosci 2009;29:7679–85.
[22] Mikulan E, Russo S, Parmigiani S, Sarasso S, Zauli FM, Rubino A, et al. Simultaneous human intracerebral stimulation and HD-EEG, ground-truth for source localization methods. Sci Data 2020;7:127. https://doi.org/10.1038/s41597-020-0467-x.
[23] Narizzano M, Arnulfo G, Ricci S, et al. SEEG assistant: a 3DSlicer extension to support epilepsy surgery. BMC Bioinf 2017;18(124):1–13.
[24] Desikan RS, Ségonne F, Fischl B, Quinn BT, Dickerson BC, Blacker D, et al. An automated labeling system for subdividing the human cerebral cortex on MRI scans into gyral based regions of interest. Neuroimage 2006;31:968–80.
[25] Pigorini A, Sarasso S, Proserpio P, Szymanski C, Arnulfo G, Casarotto S, et al. Bistability breaks-off deterministic responses to intracortical stimulation during non-REM sleep. Neuroimage 2015;112:105–13. https://doi.org/10.1016/j.neuroimage.2015.02.056.
[26] Rosanova M, Fecchio M, Casarotto S, Sarasso S, Casali AG, Pigorini A, et al. Sleep-like cortical OFF-periods disrupt causality and complexity in the brain of unresponsive wakefulness syndrome patients. Nat Commun 2018;9:1–10.
[27] Keller CJ, Honey CJ, Entz L, Bickel S, Groppe DM, Toth E, et al. Corticocortical evoked potentials reveal projectors and integrators in human brain networks. J Neurosci 2014;34:9152–63. https://doi.org/10.1523/JNEUROSCI.4289-13.2014.
[28] Trebaul L, Deman P, Tuyisenge V, Jedynak M, Hugues E, Rudrauf D, et al. Probabilistic functional tractography of the human cortex revisited. Neuroimage 2018;181:414–29. https://doi.org/10.1016/j.neuroimage.2018.07.039.
[29] Matsumoto R, Nair DR, LaPresto E, Najm I, Bingaman W, Shibasaki H, et al. Functional connectivity in the human language system: a cortico-cortical evoked potential study. Brain 2004;127:2316–30. https://doi.org/10.1093/brain/awh246.
[30] Delorme A, Makeig S. EEGLAB: an open source toolbox for analysis of single-trial EEG dynamics including independent component analysis. J Neurosci Methods 2004;134:9–21.
[31] Appelhoff S, Sanderson M, Brooks T, van Vliet M, Quentin R, Holdgraf C, Chaumon M, Mikulan E, Tavabi K, Höchenberger R, Welke D, Brunner C, Rockhill A, Larson E, Gramfort A, Jas M. MNE-BIDS: organizing electrophysiological data into the BIDS format and facilitating their analysis. JOSS 2019;4:1896. https://doi.org/10.21105/joss.01896.
[32] Mikulan E, Russo S, Zauli FM, d'Orio P, Parmigiani S, Favaro J, et al. A comparative study between state-of-the-art MRI deidentification and AnonyMI. a new method combining re-identification risk reduction and geometrical preservation 2021;42(17):5523–34.
[33] Dubarry A-S, Badier J-M, Trébuchon-Da Fonseca A, Gavaret M, Carron R, Bartolomei F, et al. Simultaneous recording of MEG, EEG and intracerebral EEG during visual stimulation: from feasibility to single-trial analysis. Neuroimage 2014;99:548–58.
[34] Badier J-M, Dubarry AS, Gavaret M, Chen S, Trébuchon AS, Marquis P, et al. Technical solutions for simultaneous MEG and SEEG recordings: towards routine clinical use. Physiol Meas 2017;38:N118.
[35] Mofakham S, Fry A, Adachi J, Stefancin PL, Duong TQ, Saadon JR, et al. Electrocorticography reveals thalamic control of cortical dynamics following traumatic brain injury. Commun Biol 2021;4:1–10.
[36] Latreille V, von Ellenrieder N, Peter-Derex L, Dubeau F, Gotman J, Frauscher B. The human K-complex: insights from combined scalp-intracranial EEG recordings. Neuroimage 2020;213:116748. https://doi.org/10.1016/j.neuroimage.2020.116748.
[37] Abramovici S, Antony A, Baldwin ME, Urban A, Ghearing G, Pan J, et al. Features of simultaneous scalp and intracranial EEG that predict localization of ictal onset zone. Clin EEG Neurosci 2018;49(3):206–12.
[38] De Stefano P, Carboni M, Marquis R, Spinelli L, Seeck M, Vulliemoz S. Increased delta power as a scalp marker of epileptic activity: a simultaneous scalp and intracranial electroencephalography study. Eur J Neurol 2022;29(1):26–35.
[39] van't Klooster MA, Zijlmans M, Leijten FS, Ferrier CH, Van Putten MJ, Huiskamp GJ. Time–frequency analysis of single pulse electrical stimulation to assist delineation of epileptogenic cortex. Brain 2011;134:2855–66.

[40] Trebaul L, Rudrauf D, Job A-S, Mălîia MD, Popa I, Barborica A, et al. Stimulation artifact correction method for estimation of early cortico-cortical evoked potentials. J Neurosci Methods 2016;264:94–102.
[41] Matsumoto R, Nair DR, LaPresto E, Bingaman W, Shibasaki H, Luders HO. Functional connectivity in human cortical motor system: a cortico-cortical evoked potential study. Brain 2006;130:181–97. https://doi.org/10.1093/brain/awl257.
[42] Crocker B, Ostrowski L, Williams ZM, Dougherty DD, Eskandar EN, Widge AS, et al. Local and distant responses to single pulse electrical stimulation reflect different forms of connectivity.NeuroImage2021;237:118094.https://doi.org/10.1016/j.neuroimage.2021.118094.
[43] Rutecki PA, Grossman RG, Armstrong D, Irish-Loewen S. Electrophysiological connections between the hippocampus and entorhinal cortex in patients with complex partial seizures. J Neurosurg 1989;70(5):667–75.
[44] Mohan UR, Watrous AJ, Miller JF, Lega BC, Sperling MR, Worrell GA, et al. The effects of direct brain stimulation in humans depend on frequency, amplitude, and white-matter proximity. Brain Stimul 2020;13:1183–95. https://doi.org/10.1016/j.brs.2020.05.009.
[45] Donos C, Mîndruță I, Ciurea J, Mălîia MD, Barborica A. A comparative study of the effects of pulse parameters for intracranial direct electrical stimulation in epilepsy. Clin Neurophysiol 2016;127:91–101. https://doi.org/10.1016/j.clinph.2015.02.013.
[46] Brocker DT, Grill WM. Principles of electrical stimulation of neural tissue. Handb Clin Neurol 2013;116:3–18.
[47] Kunieda T, Yamao Y, Kikuchi T, Matsumoto R. New approach for exploring cerebral functional connectivity: review of cortico-cortical evoked potential. Neurol Med -Chir 2015;55:374–82.
[48] Usami K, Matsumoto R, Kobayashi K, Hitomi T, Shimotake A, Kikuchi T, et al. Sleep modulates cortical connectivity and excitability in humans: direct evidence from neural activity induced by single-pulse electrical stimulation. Hum Brain Mapp 2015;36:4714–29.
[49] Lujan JL, Chaturvedi A, Choi KS, Holtzheimer PE, Gross RE, Mayberg HS, et al. Tractography-activation models applied to subcallosal cingulate deep brain stimulation. Brain Stimul 2013;6:737–9.
[50] Riva-Posse P, Choi KS, Holtzheimer PE, McIntyre CC, Gross RE, Chaturvedi A, et al. Defining critical white matter pathways mediating successful subcallosal cingulate deep brain stimulation for treatment-resistant depression. Biol Psychiatr 2014;76:963–9.
[51] Basu I, Robertson MM, Crocker B, Peled N, Farnes K, Vallejo-Lopez DI, et al. Consistent linear and non-linear responses to invasive electrical brain stimulation across individuals and primate species with implanted electrodes. Brain Stimul 2019;12:877–92. https://doi.org/10.1016/j.brs.2019.03.007.
[52] McIntyre CC, Savasta M, Walter BL, Vitek JL. How does deep brain stimulation work? Present understanding and future questions. J Clin Neurophysiol 2004;21:40–50.
[53] Slopsema JP, Peña E, Patriat R, Lehto LJ, Gröhn O, Mangia S, et al. Clinical deep brain stimulation strategies for orientation-selective pathway activation. J Neural Eng 2018;15:056029. https://doi.org/10.1088/1741-2552/aad978.
[54] Stiso J, Khambhati AN, Menara T, Kahn AE, Stein JM, Das SR, et al. White matter network architecture guides direct electrical stimulation through optimal state transitions. Cell Rep 2019;28:2554–66. https://doi.org/10.1016/j.celrep.2019.08.008. e7.
[55] Mercier MR, Bickel S, Megevand P, Groppe DM, Schroeder CE, Mehta AD, et al. Evaluation of cortical local field potential diffusion in stereotactic electroencephalography recordings: a glimpse on white matter signal. Neuroimage 2017;147:219–32.
[56] Slopsema JP, Peña E, Patriat R, Lehto LJ, Gröhn O, Mangia S, et al. Clinical deep brain stimulation strategies for orientation-selective pathway activation. J Neural Eng 2018;15. https://doi.org/10.1088/1741-2552/aad978.
[57] Reveley C, Seth AK, Pierpaoli C, Silva AC, Yu D, Saunders RC, et al. Superficial white matter fiber systems impede detection of long-range cortical connections in diffusion MR tractography. Proc Natl Acad Sci Unit States Am 2015;112(21):E2820–8.
[58] Iannetti GD, Hughes NP, Lee MC, Mouraux A. Determinants of laser-evoked EEG responses: pain perception or stimulus saliency? J Neurophysiol 2008;100:815–28.
[59] Novembre G, Pawar VM, Bufacchi RJ, Kilintari M, Srinivasan M, Rothwell JC, et al. Saliency detection as a reactive process: unexpected sensory events evoke corticomuscular coupling. J Neurosci 2018;38:2385–97.
[60] Voysey Z, Martín-López D, Jiménez-Jiménez D, Selway RP, Alarcón G, Valentín A. Electrical stimulation of the anterior cingulate gyrus induces responses similar to K-complexes in awake humans. Brain Stimul 2015;8:881–90.
[61] Somervail R, Zhang F, Novembre G, Bufacchi RJ, Guo Y, Crepaldi M, et al. Waves of change: brain sensitivity to differential, not absolute, stimulus intensity is conserved across humans and rats. Cerebr Cortex 2021;31:949–60.
[62] Fecchio M, Pigorini A, Comanducci A, Sarasso S, Casarotto S, Premoli I, et al. The spectral features of EEG responses to transcranial magnetic stimulation of the primary motor cortex depend on the amplitude of the motor evoked potentials. PLoS One 2017;12:e0184910.
[63] Casarotto S, Romero Lauro LJ, Bellina V, Casali AG, Rosanova M, Pigorini A, et al. EEG responses to TMS are sensitive to changes in the perturbation parameters and repeatable over time. PLoS One 2010;5:e10281.
[64] Ilmoniemi RJ, Kičić D. Methodology for combined TMS and EEG. Brain Topogr 2010;22:233–48.
[65] Nathan SS, Sinha SR, Gordon B, Lesser RP, Thakor NV. Determination of current density distributions generated by electrical stimulation of the human cerebral cortex. Electroencephalogr Clin Neurophysiol 1993;86:183–92.
[66] Belardinelli P, Biabani M, Blumberger DM, Bortoletto M, Casarotto S, David O, et al. Reproducibility in TMS–EEG studies: a call for data sharing, standard procedures and effective experimental control. Brain Stimul: Basic Transl Clin Res Neuromodulation 2019;12:787–90.
[67] Kundu B, Davis TS, Philip B, Smith EH, Arain A, Peters A, et al. A systematic exploration of parameters affecting evoked intracranial potentials in patients with epilepsy. Brain Stimul 2020;13:1232–44. https://doi.org/10.1016/j.brs.2020.06.002.
[68] Darmani G, Bergmann TO, Zipser C, Baur D, Müller-Dahlhaus F, Ziemann U. Effects of antiepileptic drugs on cortical excitability in humans: a TMS-EMG and TMS-EEG study. Hum Brain Mapp 2019;40(4):1276–89.
[69] Paulk AC, Zelmann R, Crocker B, Widge AS, Dougherty DD, Eskandar EN, et al. Local and distant cortical responses to single pulse intracranial stimulation in the human brain are differentially modulated by specific stimulation parameters. Brain Stimul 2022;15(2):491–508. https://doi.org/10.1016/j.brs.2022.02.017.
[70] Sporns O, Honey CJ. Small worlds inside big brains. Proc Natl Acad Sci U S A 2006 Dec 19;103(51):19219–20.
[71] Deco G, Jirsa VK, McIntosh AR. Emerging concepts for the dynamical organization of resting-state activity in the brain. Nat Rev Neurosci 2011;12:43–56.